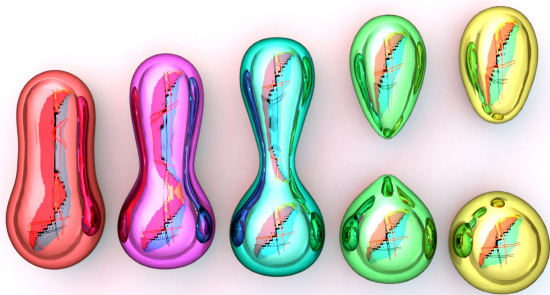


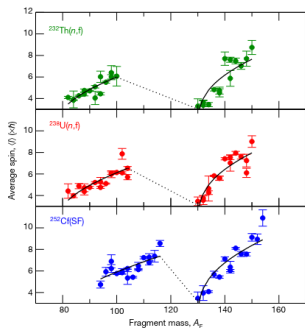
Fifth Gogny conference

Fission Fragment Spins : Understanding the Mechanisms of Their Rotation

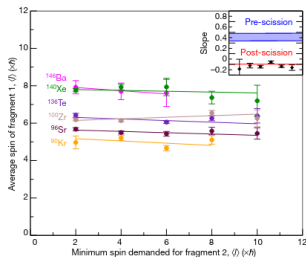
Guillaume SCAMPS



Spin of the fragments



Correlations



J. N. Wilson, Nature, 590, 566 (2021)

- The average spin follows a sawtooth shape
- No correlations between the spins of the fragments

Spins are mostly perpendicular to the fission axis

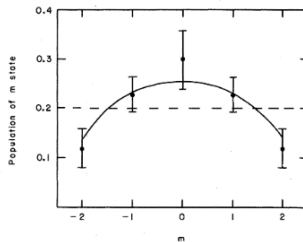


FIG. 9. The points are the calculated populations of the various m substates of the 2^+ level in ^{144}Ba . These values were determined using the fitted experimental angular distribution of the $2^+ \rightarrow 0^+$ γ ray. The solid line represents the predicted population of the m states as calculated from the statistical-model analysis of the de-excitation process using Eqs. (4) and (5) with an assumed value of $B=6$ [Eq. (3)] for the initial angular momentum distribution.

J. B. Wilhelmy, E. Cheifetz, R. C. Jared, S. G. Thompson, H. R. Bowman, and J. O. Rasmussen Phys. Rev. C 5, 2041 (1972)

Literature

- Thermal excitations
- Quantum fluctuations
- Coulomb force
- Breaking of the neck

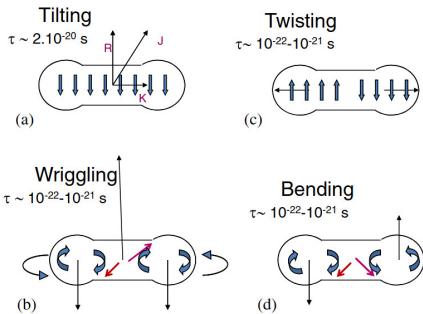
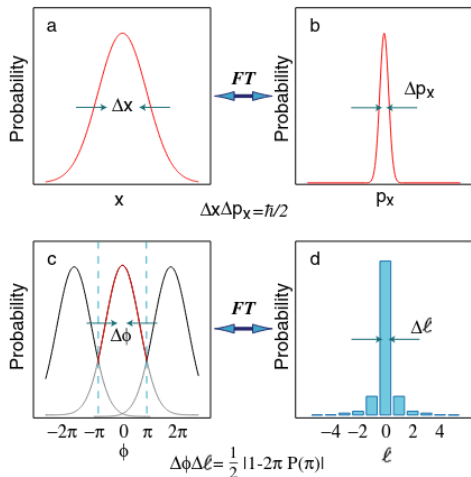
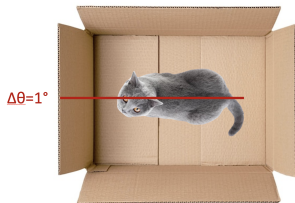
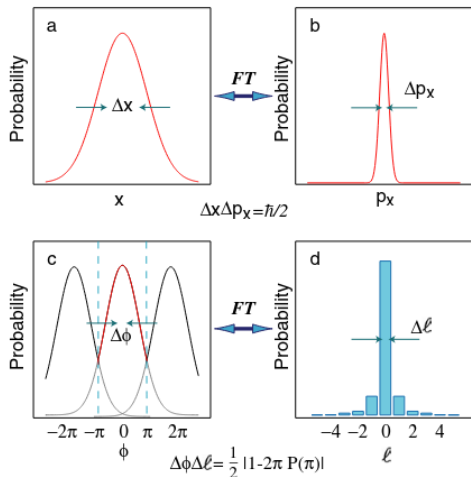


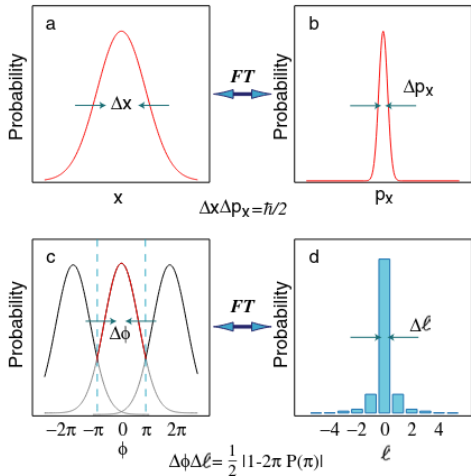
Illustration from B. John, *J. Phys.*, 85, 2, (2015).



S. Franke-Arnold, et al. New Journal of Physics 6, 103 (2004)

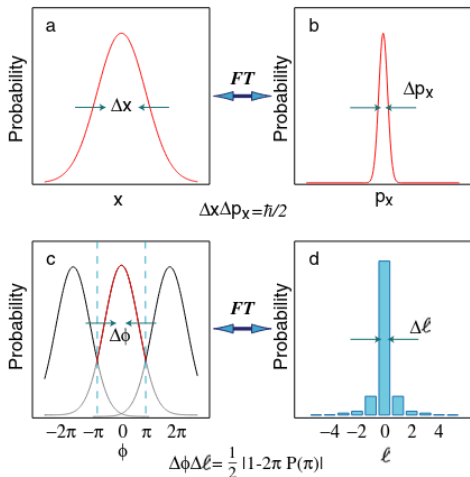


S. Franke-Arnold, et al. New Journal of Physics 6, 103 (2004)



For $\Delta\Theta = 1^\circ$, $\Delta L = 56\hbar$.
 For a cat, angular velocity
 $\omega = 10^{-33} \text{ s}^{-1}$

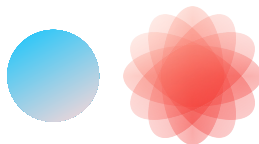
S. Franke-Arnold, et al. New Journal of Physics 6, 103 (2004)



S. Franke-Arnold, et al. *New Journal of Physics* 6, 103 (2004)

Orientation pumping mechanism

Isotropic potential at scission



Confining potential at scission

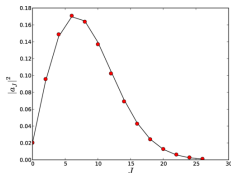


I.N Mikhailov, P Quentin, *PLB* 462 (1999).

For $\Delta\Theta = 1^\circ$, $\Delta L = 56\hbar$.

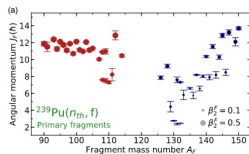
For a nucleus, angular velocity
 $\omega = 10^{20} \text{s}^{-1}$

Static HFB



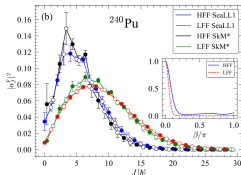
G. F. Bertsch, T. Kawano, and L. M. Robledo, PRC 99, 034603 (2019)

Scission configuration



P. Marević, N. Schunck, J. Randrup, and R. Vogt PRC 104, L021601 (2021).

TDHFB - TDSLDA

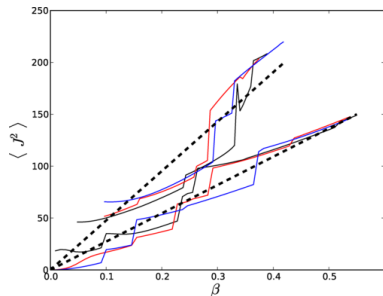


A. Bulgac, et al., PRL 126, 142502 (2021)

Projection method

$$|a_J^F|^2 = \frac{2J+1}{2} \int_0^{2\pi} \sin(\beta)$$

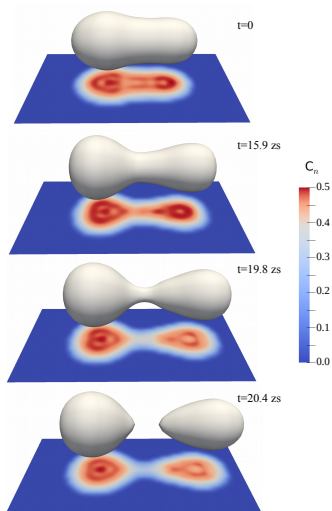
$$P_J(\cos(\beta)) \langle \Psi | e^{-iJ_x^F \beta / \hbar} | \Psi \rangle$$



G. F. Bertsch, T. Kawano, and L. M. Robledo,
PRC 99, 034603 (2019)

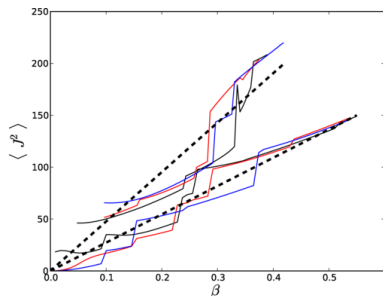
Problem of interpretation

- The spin cut-off distribution is already present in the ground state of even-even deformed nuclei if symmetry are not restored
- \hat{J}^2 and $\hat{P}(J)$ are 2 and N-body operators
- Fragments do not rotate in dynamical approaches



Problem of interpretation

- The spin cut-off distribution is already present in the ground state of even-even deformed nuclei if symmetry are not restored
- \hat{J}^2 and $\hat{P}(J)$ are 2 and N-body operators
- Fragments do not rotate in dynamical approaches



G. F. Bertsch, T. Kawano, and L. M. Robledo,
PRC 99, 034603 (2019)

Problem of interpretation

- The spin cut-off distribution is already present in the ground state of even-even deformed nuclei if symmetry are not restored
- \hat{J}^2 and $\hat{P}(J)$ are 2 and N-body operators
- Fragments do not rotate in dynamical approaches

Uncertainty principle ?

If the overlap is gaussian

$$\langle \Psi | \hat{R}(\theta) | \Psi \rangle = e^{-\frac{\theta^2}{2\sigma_\theta^2}}$$

The projection gives,

$$P(J) = \frac{2J+1}{2\sigma_J^2} e^{-\frac{J(J+1)}{2\sigma_J^2}}$$

with $\sigma_J \sigma_\theta = 1$

$^{144}\text{Ba} + ^{96}\text{Sr}$ at 16 Fm, $\Theta_{ini}=25$ deg, Functional : Skyrme Sly4d

$J_y(x, z)[\hbar \text{ fm}^{-3}]$

G. Scamps, PRC 106, 054614 (2022).

One body-evolution - One body-observable

$^{144}\text{Ba} + ^{96}\text{Sr}$ at 16 Fm, $\Theta_{ini}=25$ deg, Functional : Skyrme Sly4d

$J_y(x, z)[\hbar \text{ fm}^{-3}]$

G. Scamps, PRC 106, 054614 (2022).

One body-evolution - One body-observable

$^{144}\text{Ba} + ^{96}\text{Sr}$ at 16 Fm, $\Theta_{ini} = 25$ deg, Functional : Skyrme Sly4d

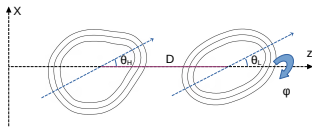
$J_y(x, z)[\hbar \text{ fm}^{-3}]$

G. Scamps, PRC 106, 054614 (2022).

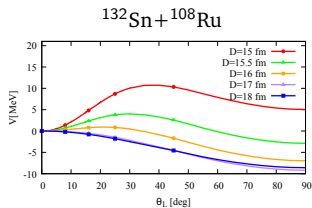
$^{144}\text{Ba} + ^{96}\text{Sr}$ at 16 Fm, $\Theta_{ini} = 25$ deg, Functional : Skyrme Sly4d

$J_y(x, z)[\hbar \text{ fm}^{-3}]$

G. Scamps, PRC 106, 054614 (2022).



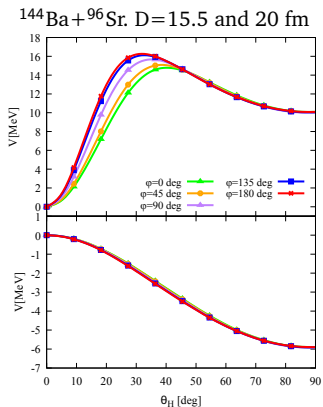
Potential as a function of the light fragment angle



Two torques :

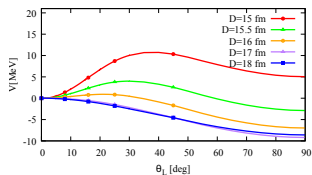
- attractive nucleus-nucleus torque
- repulsive Coulomb torque

Potential as a function of the light fragment angle



The azimuthal angle doesn't have an important role.

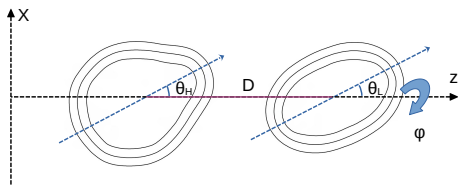
Frozen Hartree-Fock potential



Two torques :

- attractive nucleus-nucleus torque
- repulsive Coulomb torque

4 degrees of freedom



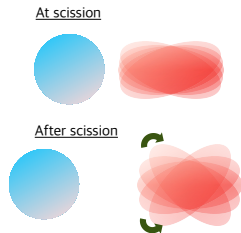
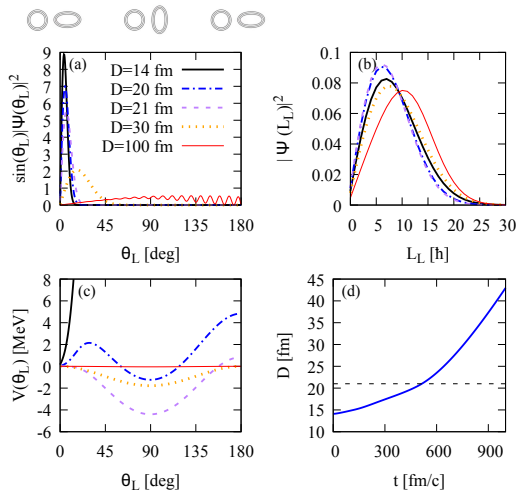
Hamiltonian

$$\hat{H}(D) = \frac{\hbar^2}{2I_H} \hat{L}_H^2 + \frac{\hbar^2}{2I_L} \hat{L}_L^2 + \frac{\hbar^2}{2I_\Lambda(D)} \hat{\Lambda}^2 + \hat{V}(\hat{\Theta}_H, \hat{\Theta}_L, \hat{\varphi}, D)$$

Solved in basis $|L_H, m, L_L, -m\rangle$

G. Scamps, G. Bertsch, Phys. Rev. C 108, 034616(2023).

Similar to the orientation pumping mechanism model Mikhailov, I. N., and Quentin, P. Physics Letters B, 462(1-2), 7-13 (1999)



G. Scamps, G. Bertsch, Phys. Rev. C 108, 034616 (2023).

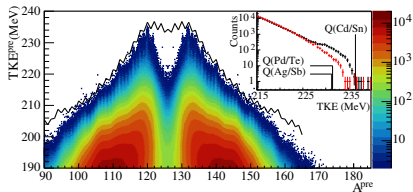
Effect of quadrupole deformation \gg effect of $Z_1 Z_2$

TABLE II. Average spin $\langle L^2 \rangle^{\frac{1}{2}}$ in unit of \hbar for the three fission fragments at scission ($D = 21$ fm) and at large distances. The last two columns show the same quantity with an MOI divided by 2.

Nucleus	Scission	Final	Scission ($I_{\frac{1}{2}}$)	Final ($I_{\frac{1}{2}}$)
^{108}Ru	9.28	12.31	7.24	10.38
^{144}Ba	10.04	10.95	7.70	8.66
^{96}Sr	7.74	9.30	6.03	7.62

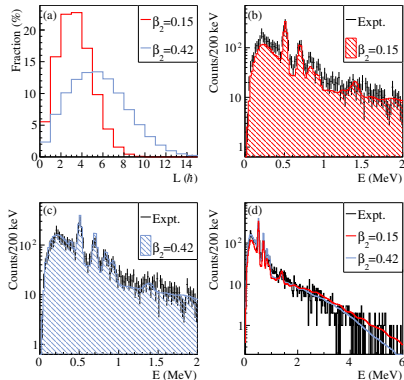
also J. Randrup, PRC 108, 064606 (2023) : increase of 1 to 3 \hbar due to the Coulomb torque.

Cold fission selection TXE < 8 MeV



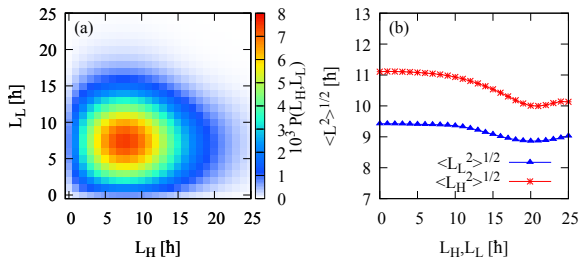
Results

- ^{132}Sn is found in ground-state
- The collective Hamiltonian model with $\beta_2=0.42$ reproduces the experimental γ -spectrum

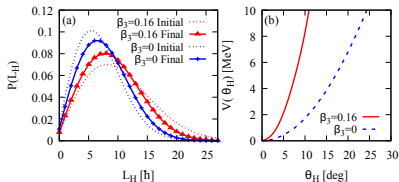
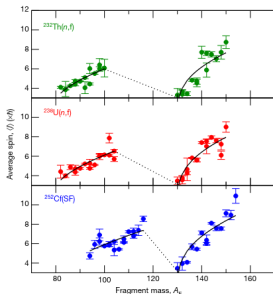
 γ -spectrum

A. Francheteau, L. Gaudefroy, G. Scamps, O. Roig, V. Méot, A. Ebran, and G. Bélier, PRL 132, 142501 (2024).

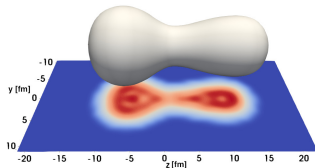
Correlation between the angular momentum

 $^{144}\text{Ba} + ^{96}\text{Sr}$

- No or small correlation observed in the magnitude of the angular momentum.
- More angular momentum for the heavy fragment



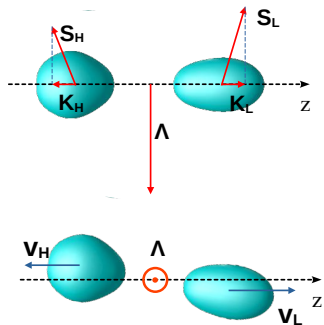
Mechanism



- Pear-shaped deformation plays an important role at scission. G. Scamps C. Simenel, Nature 564, pages 382–385 (2018)
- Octupole deformation makes the angular potential stiffer which increase the zero-point motion \rightarrow more angular momentum

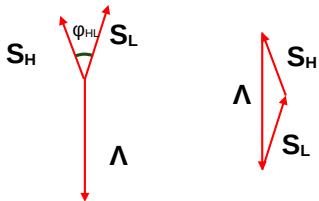
G. Scamps, G. Bertsch, Phys. Rev. C 108, 034616 (2023).

Orbital angular momentum

In spontaneous fission of a 0^+ state

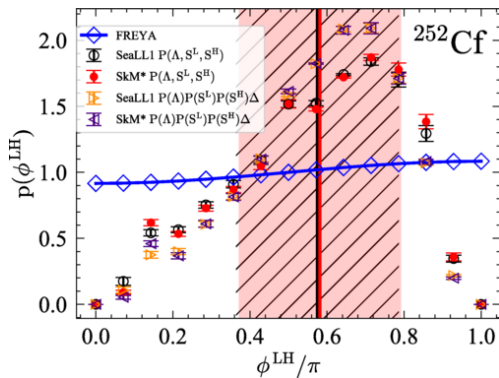
$$\mathbf{S}_H + \mathbf{S}_L + \mathbf{\Lambda} = 0,$$

Triangular rule :

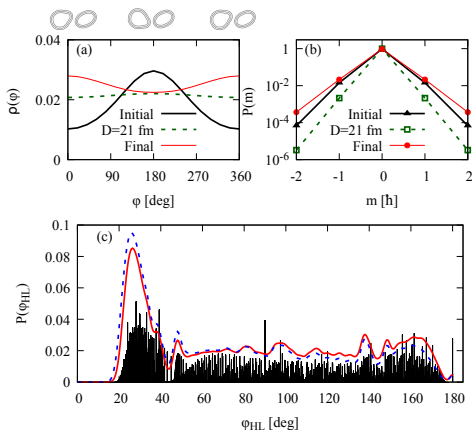


$$\cos(\varphi_{HL}) = \left(\frac{\Lambda(\Lambda + 1) - S_H(S_H + 1) - S_L(S_L + 1)}{2\sqrt{S_H(S_H + 1)S_L(S_L + 1)}} \right)$$

TDDFT (in 2022) vs Freya



A. Bulgac, I. Abdurrahman, K. Godbey, and I. Stetcu, Phys. Rev. Lett. 128, 022501(2022).



Geometry

- Small azimuthal correlation
- Spin are perpendicular to the fission axis
- Complex pattern in the opening angle, different from previous model

G. Scamps, G. Bertsch, Phys. Rev. C 108, 034616 (2023).

Projection method

Projection on the spin and K number (Projection of the spin on the fission axis)

$$\hat{P}_{MK}^S = \frac{(2S+1)}{16\pi^2} \int d\Omega \mathcal{D}_{MK}^{S*}(\Omega) e^{i\alpha\hat{S}_z} e^{i\beta\hat{S}_y} e^{i\gamma\hat{S}_z},$$

$$P(S_F, K_F) = \langle \Psi | \hat{P}_{K_F K_F}^{S_F} | \Psi \rangle,$$

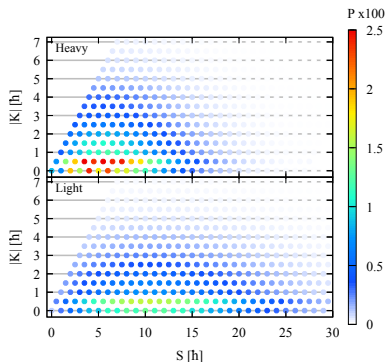
Calculation of the overlap : G. F. Bertsch and L. M. Robledo, PRL 108, 042505 (2012)

$$\langle \Psi | \hat{R} | \Psi \rangle = \frac{(-1)^n}{\prod_{\alpha}^n v_{\alpha}^2} \text{pf} \begin{bmatrix} V^T U & V^T R^T V^* \\ -V^{\dagger} R V & U^{\dagger} V^* \end{bmatrix}$$

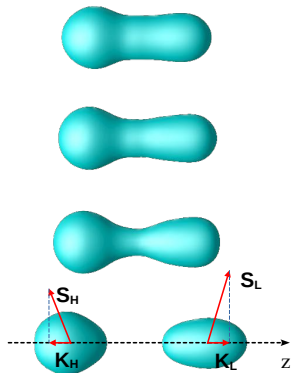
Optimized Pfaffian calculation : M. Wimmer, ACM Trans. Math Softw. 38, 30 (2012).

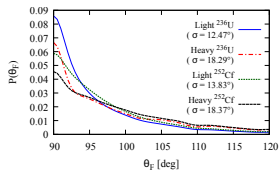
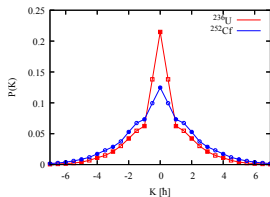
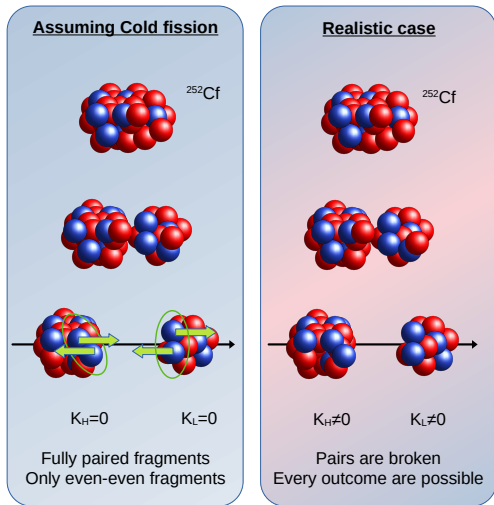
Spin distribution in the fragments

Obtained using 3-angle projection operator



Geometry of the reaction





$$\cos \theta_F = \frac{K_F}{\sqrt{S_F(S_F + 1)}}$$

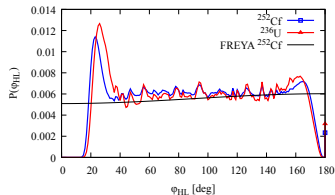
G.scamps, I. Abdurrahman, M. Kafker, A. Bulgac, and I. Stetcu, PRC 108 (6), L061602.

$$\varphi_{HL} = \arccos \left(\frac{\Lambda(\Lambda + 1) - S_H(S_H + 1) - S_L(S_L + 1)}{2\sqrt{S_H(S_H + 1)S_L(S_L + 1)}} \right)$$

$$P(\Lambda, S_H, S_L) = \sum_{k_H k_L} \langle \Psi | \hat{P}_{0,0}^\Lambda \hat{P}_{k_H k_H}^{S_H} \hat{P}_{k_L k_L}^{S_L} | \Psi \rangle.$$

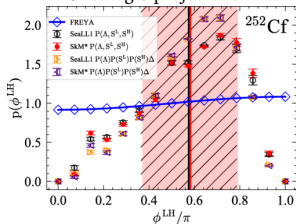
$$P(\Lambda, S_H, S_L) = \sum_{K_H K_L K'_H K'_L} (-1)^{K'_H - K_H + K'_L - K_L}$$

$$C_{S_H, -K_H, S_L, -K_L}^{\Lambda, 0} C_{S_H, -K'_H, S_L, -K'_L}^{\Lambda, 0} \langle \Psi | \hat{P}_{K_H K'_H}^{S_H} \hat{P}_{K_L K'_L}^{S_L} | \Psi \rangle$$



G.scamps, I. Abdurrahman, M. Kafker, A. Bulgac, and I. Stetcu, PRC 108 (6), L061602.

One angle projector :



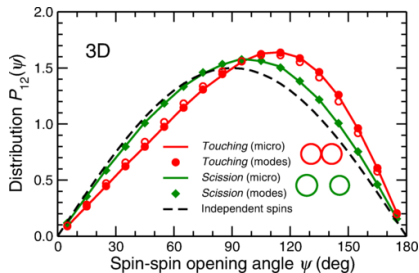
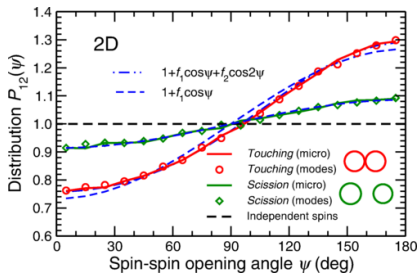
Main points

- Orientation-pumping (uncertainty principle) mechanism at scission
- Additional effect of the Coulomb torque
- Internal excitation (breaking of pairs)
- Spins are mainly perpendicular to the fission axis
- Uncorrelated magnitude and orientation of the spins
- Dependence of the mechanism with the deformation (quadrupole and octupole)

Outlook

- TD-GCM with rotated fragments
- Rotated fission system

Thank you

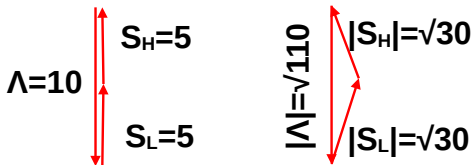


J. Randrup, Phys. Rev. C 106, L051601 (2022).

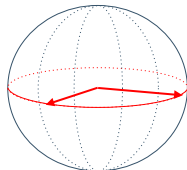
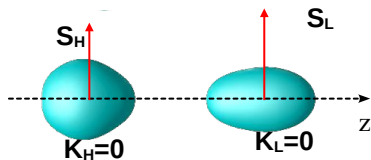
Question

- How the quantal effects change this picture ?
- How the geometry change the opening angle distribution assuming no correlation ?

Non alignment of the spins

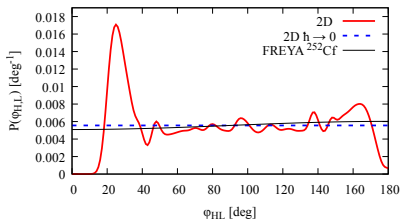


To get a 5 degrees angle between two spins require spins of $262 \hbar$ and $6565 \hbar$ for 1 degree

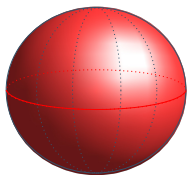
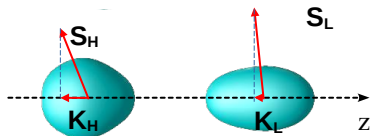


$$|\psi\rangle = \sum_{S_H, K_H, S_L, K_L} c_{S_H, K_H, S_L, K_L} |S_H, K_H, S_L, K_L\rangle,$$

$$|c_{S_H, K_H, S_L, K_L}|^2 \propto \delta_{K_H, 0} \delta_{K_L, 0} (2S_H + 1) e^{\frac{-S_H(S_H+1)}{2\sigma_H^2}} \times (2S_L + 1) e^{\frac{-S_L(S_L+1)}{2\sigma_L^2}}.$$

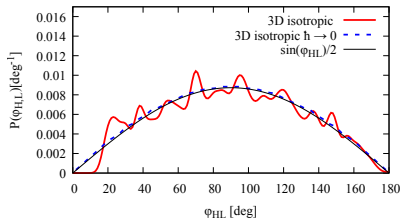


G. Scamps, PRC 109, L011602 (2024).

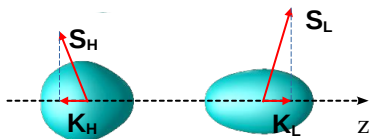


$$|\psi\rangle = \sum_{S_H, K_H, S_L, K_L} c_{S_H, K_H, S_L, K_L} |S_H, K_H, S_L, K_L\rangle,$$

$$|c_{S_H, K_H, S_L, K_L}|^2 \propto e^{\frac{-S_H(S_H+1)}{2\sigma_H^2}} e^{\frac{-S_L(S_L+1)}{2\sigma_L^2}}.$$

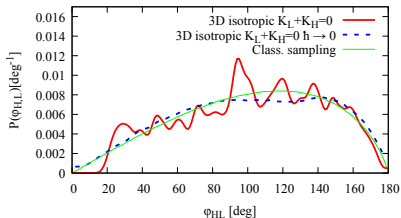
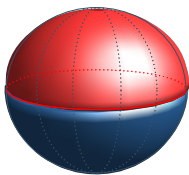


G. Scamps, PRC 109, L011602 (2024).

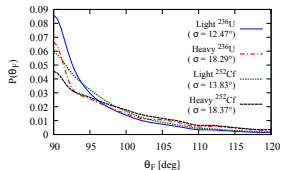
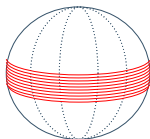
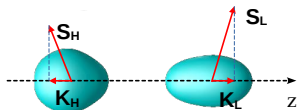


$$|\psi\rangle = \sum_{S_H, K_H, S_L, K_L} c_{S_H, K_H, S_L, K_L} |S_H, K_H, S_L, K_L\rangle,$$

$$|c_{S_H, K_H, S_L, K_L}|^2 \propto \delta_{K_H - K_L} e^{-\frac{S_H(S_H+1)}{2\sigma_H^2}} e^{-\frac{S_L(S_L+1)}{2\sigma_L^2}}.$$

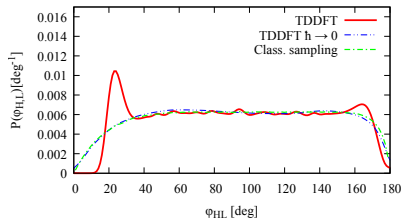


G. Scamps, PRC 109, L011602 (2024).



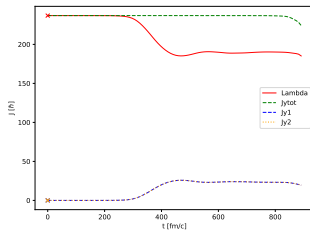
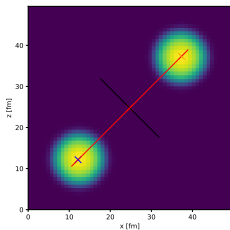
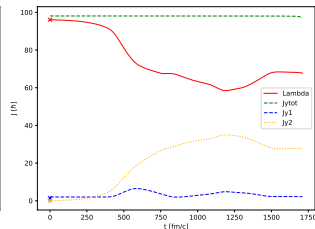
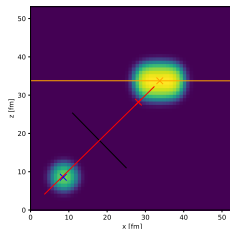
$$|\Psi\rangle = \sum_{S_H, K_H, S_L, K_L} c_{S_H, K_H, S_L, K_L} |S_H, K_H, S_L, K_L\rangle,$$

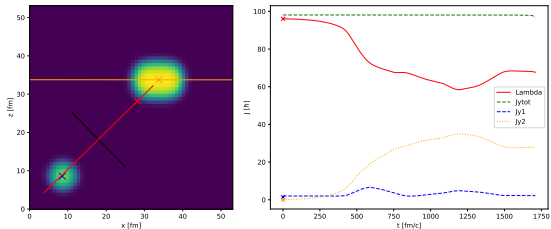
$|c_{S_H, K_H, S_L, K_L}|^2$ From TDDFT

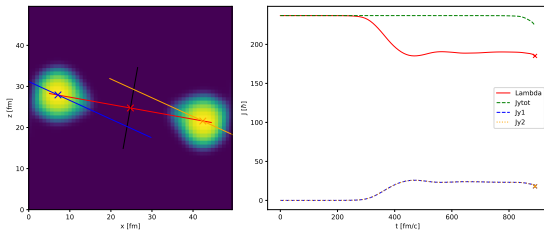


TDDFT shows an intermediate case between 2D and 3D.

G. Scamps, PRC 109, L011602 (2024).

$^{208}\text{Pb} + ^{208}\text{Pb}$

 $^{50}\text{Ca} + ^{176}\text{Yb}$


$^{208}\text{Pb} + ^{208}\text{Pb}$
 $^{50}\text{Ca} + ^{176}\text{Yb}$


$^{208}\text{Pb} + ^{208}\text{Pb}$

 $^{50}\text{Ca} + ^{176}\text{Yb}$